$p + A$ Physics in an EIC Fixed-Target Setup

R. Vogt

Nuclear and Chemical Sciences Division, Lawrence Livermore National Laboratory, Livermore, CA 94551, USA
Physics and Astronomy Department, University of California, Davis, CA 95616, USA

based on:
C. J. Naim *et al.*, arXiv:2603.00265, submitted to Phys. Rev. D
F. Arleo *et al.*, arXiv:2506.17554, Phys. Rev. C 113 (2026) 040501

Figure 1: **This work was performed under the auspices of the U.S. Department of Energy by Lawrence Livermore National Laboratory under Contract DE-AC52-07NA27344 and supported by the U.S. Department of Energy, Office of Science, Office of Nuclear Physics (Nuclear Theory) under contract number DE-SC-0004014 and the HEFTY Collaboration.**

A Fixed-Target Program at the EIC

Conceptual notion of the EIC collision region with a fixed target

In the A-going direction (left) particle from fixed target $p + A$ and $A + A'$ collisions can be measured, top energy of $\sqrt{s_{NN}} \sim 14$ GeV for 100 GeV/nucleon Au beam

Cross sections for space radiation protection can also be measured, as discussed by von Doetinchem and Brown

Either a gas jet target (like SMOG@LHCb) or target wires (like STAR BES II) can be used; likely target wires in ePIC

See the white paper, arXiv:2603.00265, and workshop website https://indico.cfnssbu.physics.sunysb.edu/event/496/

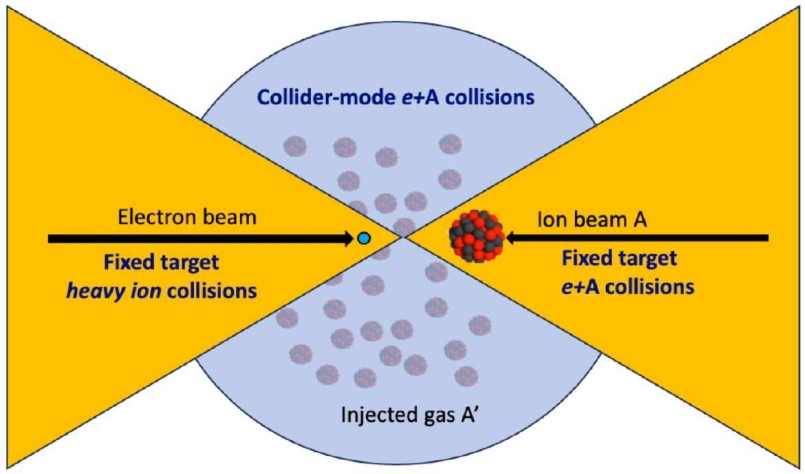

Focus in this Talk is on the Potential $p + A$ Program

.

Putting the Possible Energy Range Into Perspective

The maximum energy of the proton beam is 250 GeV; minimum is in principle the injection energy, giving a range of potential $p + A$ energies, $\sqrt{s_{NN}} \sim 7 - 21.7$ GeV.

This range is bigger than that planned for NA60+ at the SPS and covers the lower range of NA50 to well below the energy of E906 (SeaQuest, $p_{\mathrm{beam}} = 120$ GeV)

In addition to cold matter studies, these measurements would provide the missing baseline from at least some of the STAR Beam Energy Scan II measurements

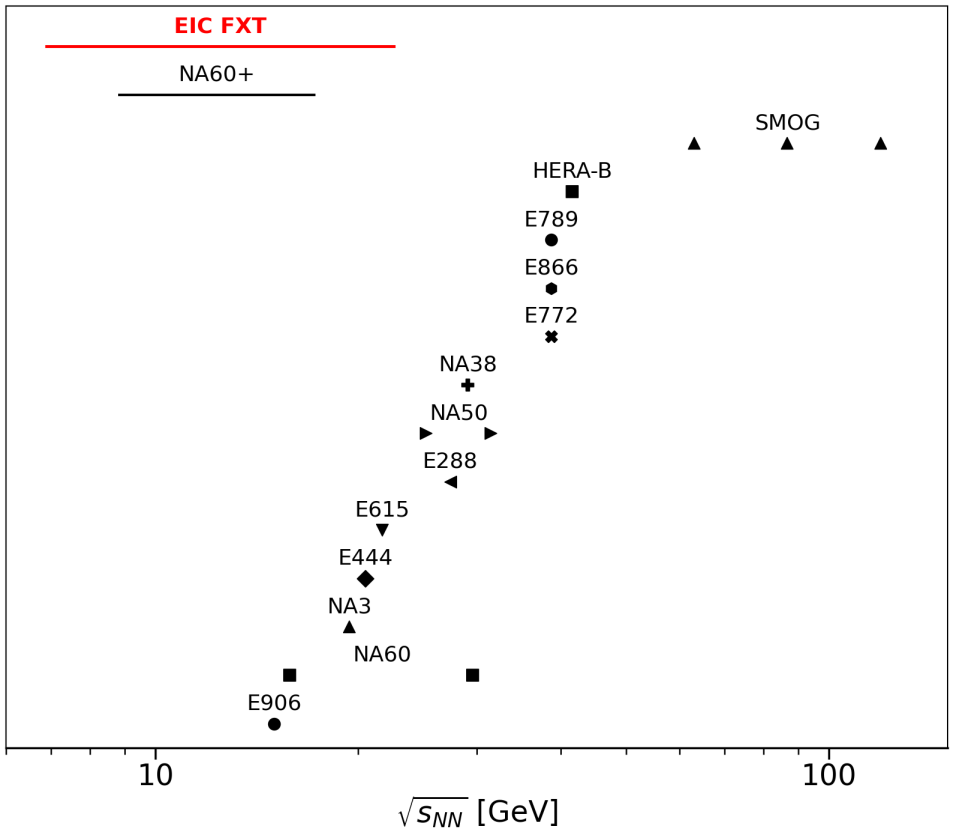

Target Wires vs. Gas Jet Target?

Target Wires (STAR BES II runs)

- **Wires have to be installed and left in place**
- **Target wheel could add multiple potential targets**
- **Can't be run parasitically, separate runs required to steer beam onto the targets**

Gas Jet (LHCb SMOG setup)

- **The SMOG device uses noble or neutral gases (^{4}He, Ne, Ar (Kr, Xe possible) and H_2, O_2, and N_2)**
- **Gases can be continuously injected and changed easily**
- **Can be run parasitically, LHCb has collected large datasets with the new SMOG2 setup**

Advantages to both but ideally more than one single target would be used: a lever arm in A is useful, both for understanding cold matter effects and for space radiation studies (C, Si, Al preferred relative to Au)

Putting Target Wires in ePIC

Placing the target in the backward region ($z = -3290$ mm relative to the interaction point) exploits the forward detector systems

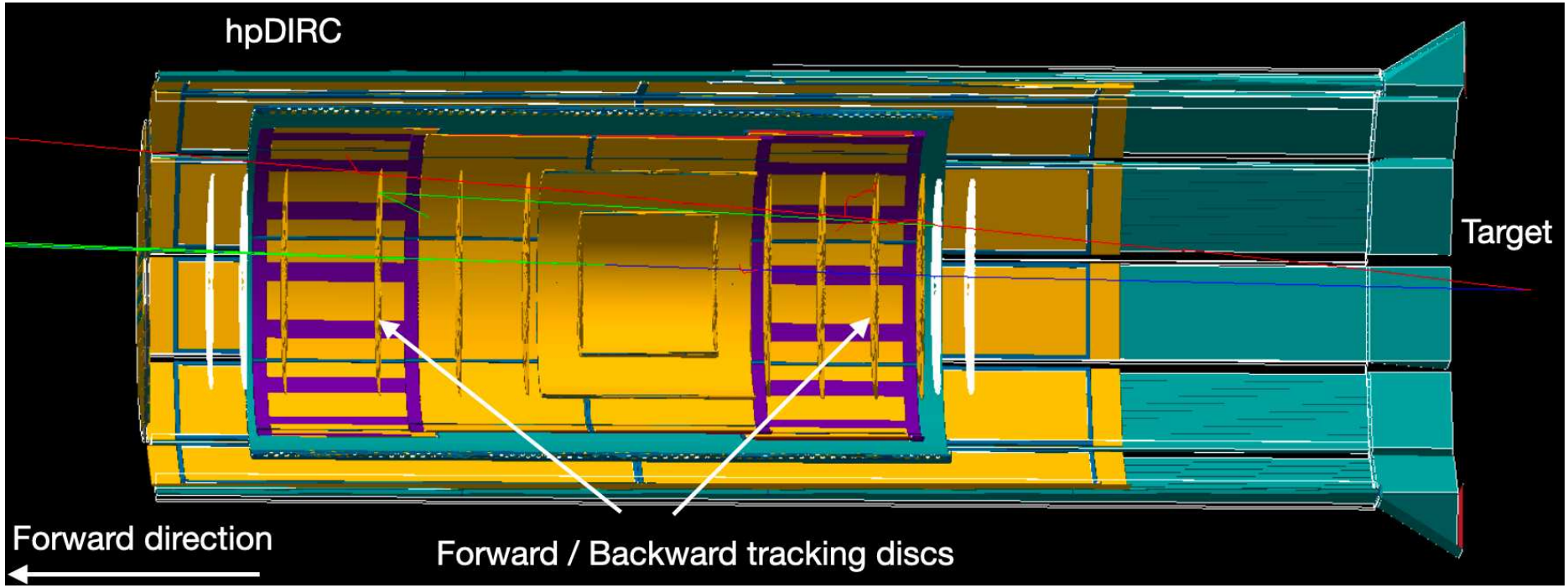

Some Idealized Example Simulations

Simulations in arXiv:2603.00265 assumed $p + p$ collisions for simplicity

A 200 GeV proton beam was assumed for $\sqrt{s} = 19.4$ GeV

Studied charged pion and J/ψ acceptance, with pion and muon (from J/ψ decays) tracks with at least 4 hits in the tracker

Pion acceptance in η and p_T studied for two different target positions

J/ψ acceptance in m_T and x_2 studied for single target posiiton

ePIC Phase Space Coverage Depends on Target Location

Placing the target in the backward region ($z = -3290$ mm relative to the interaction point) exploits the forward detector systems

With target in the backward region, left, acceptance is forward of midrapidity, reaches lower x_2 (and higher p_T) but may be less useful as baseline for STAR BES II

Putting the target at $z = 0$ (at the reaction point), right, would allow measurements closer to midrapidity but generally at lower p_T

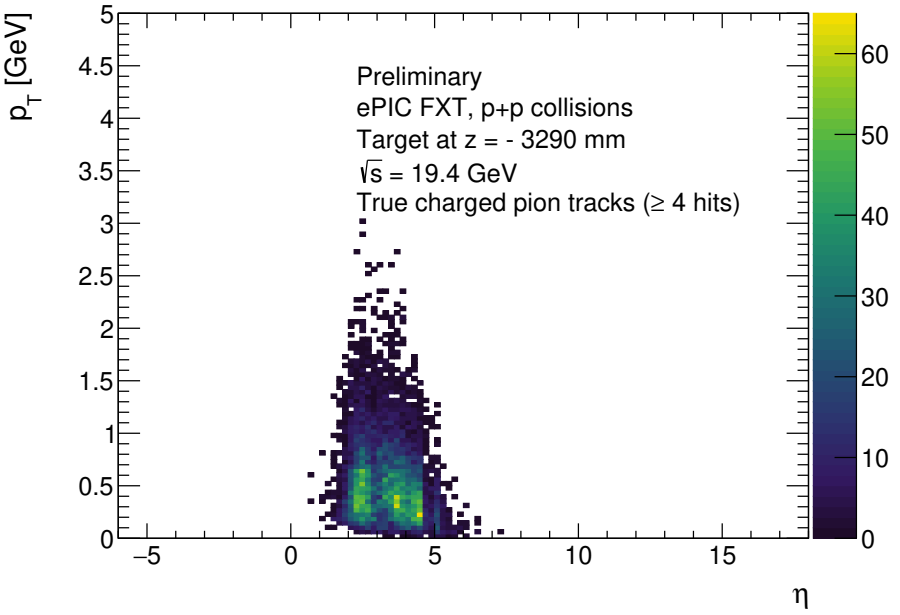

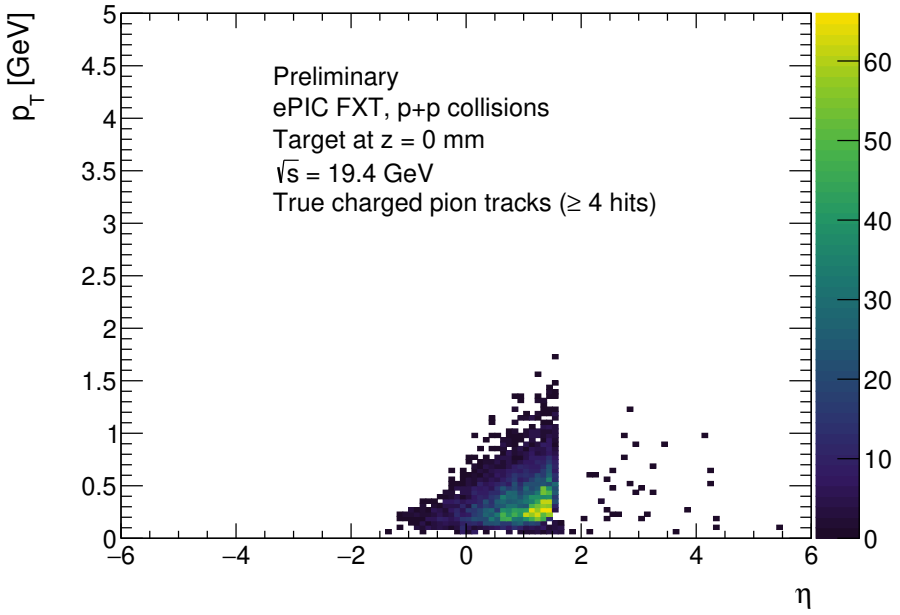

J/ψ x_2 Coverage

In the configuration where the target is backward of the interaction point, $0.02 < x_2 < 0.4$**, in the antishadowing region,** $m_T \sim 4.5$ **GeV implies** $p_T \sim 3.5$ **GeV**

With the target at the interaction point, x_2 **would be larger**

Going to lower energies would move acceptance to higher x_2**, lower** m_T**, as well as changing the balance of production from** gg **dominated (still) at the higher energy to** $q\overline{q}$ **dominance at the low energy end of** $\sqrt{s_{NN}}$ **range**

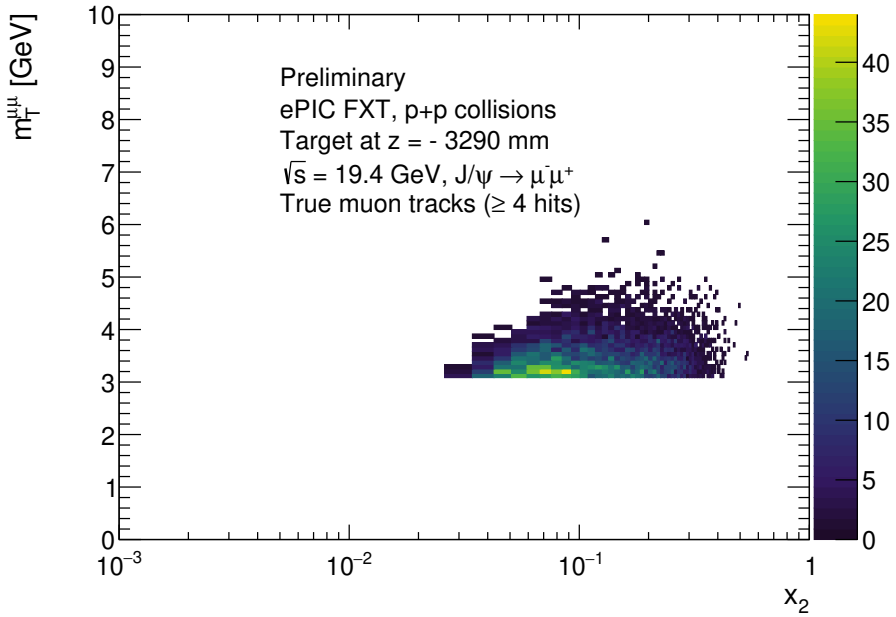

Using the EIC to Disentangle (Really Cold) Nuclear Matter Effects

.

Cold Nuclear Matter Effects: from the LHC to the EIC

F. Arleo *et al.*, Phys. Rev C 113 (2026) 040501

CFNS workshop, January 2025: https://indico.cfnssbu.physics.sunysb.edu/event/338/

White paper, arXiv:2506.17454, identified key questions and discussed how to address them – now first published PRC Perspectives article

- **Current Data**
- **Leading-Twist nPDF Effects vs. Saturation**
- **Energy Loss in Cold Nuclear Matter**
- **Nuclear Absorption**
- **Other Effects**
  - **Comovers (quarkonium)**
  - **Impact Parameter Dependence of nPDF Effects**
  - **Intrinsic Heavy Flavors (heavy flavors)**
- **Future Experiments**

Some contributions from the paper are now discussed in the context of the fixed-target potential at the EIC

Example: Cold Matter Effects on Quarkonium

Perturbative QCD production cross section in $p+A$ collisions

$$\sigma_{pA}^{\rm pQCD}(S,m^2) \;=\; \sum_{i,j=q,\overline{q},g}\int_{4m_Q^2/S}^1 \frac{d\tau}{\tau}\int d^2b dz d\epsilon\, dx_1\, dx_2\, \delta(x_1x_2-\tau)\delta(x'_F-x_F-\delta x_F(\epsilon))\delta(x'_F-x_1+x_2)$$
$$\times P(\epsilon)\, S_A^{\rm abs}(\vec{r},z)\, S_{\rm co}(\tau)\, f_i^p(x_1,\mu_F^2,k_T^p) F_i^A(x'_1,\mu_F^2,k_T^A,\vec{b},z)\,\widehat{\sigma}_{ij}(s,m^2,\mu_F^2,\mu_R^2)$$

Survival probability for absorption of a (proto)charmonium state in nuclear matter

$$S_A^{\rm abs}(b,z) = \exp\left\{-\int_z^\infty dz'\rho_A(b,z')\sigma_{\rm abs}(z-z')\right\}$$

$S^{\rm co}$ is the survival probability for quarkonium interactions with comovers

$P(\epsilon)$ is energy loss probability that modifies the x_F of the produced J/ψ state; k_T broadening can be combined with energy loss

Nuclear parton densities, including centrality dependence

$$F_i^A(x,Q^2,\vec{b},z) = \rho_A(s) S^i(A,x,Q^2,k_T,\vec{b},z) f_i^p(x,Q^2)\;;\quad s=\sqrt{b^2+z^2}\;;\quad \rho_A(s)=\rho_0\frac{1+\omega(s/R_A)^2}{1+\exp[(s-R_A)/d]}$$

S^i is nPDF effect on parton i; no nuclear modification, $S^i(A,x,Q^2,\vec{r},z)\equiv 1$

Intrinsic heavy flavor production added to NLO pQCD cross section

$$\sigma_{pA}^{\rm tot} \;=\; \sigma_{pA}^{\rm pQCD} + \sigma_{pA}^{\rm iQ}$$

One can compile similarly modified cross sections for other observables

Nuclear PDF Effects (nPDFs) vs. Saturation

x_2 is too Large for Saturation Physics to Apply in Fixed-Target Mode

.

nPDF effects are not the whole story for J/ψ

If nPDFs are sufficient to explain J/ψ data, then the results should be independent of $\sqrt{s_{NN}}$ and depend only on x_2

(Left) J/ψ data from fixed-target energies to the LHC. The x_2 range is wide and results are very different, with experiments that reach large x_F showing the strongest modification – this region could be further explored in an EIC fixed-target configuration

(Right) The EPPS16 gluon ratio for W/Be compared to the E866 results at $\sqrt{s_{NN}} = 38.7$ GeV. The EPPS16 results lie consistently above the data.

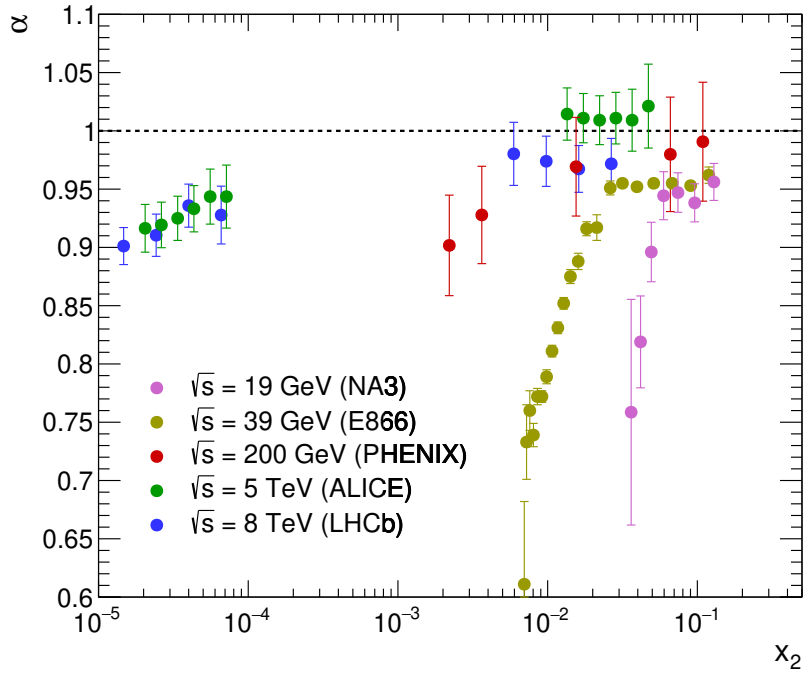

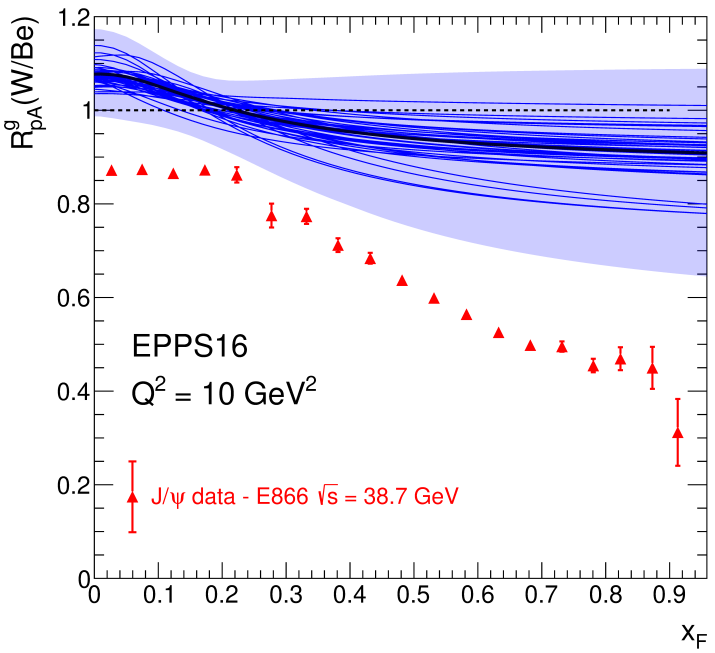

x and Q^2 range

DIS and Drell-Yan fixed-target data cover an x and Q^2 range that does not reach into the saturation regime.

The EIC kinematic reach in collider model will be greater and reach higher Q^2, putting the saturation regime within reach for heavy nuclei, although not penetrating far into it

The EIC kinematic reach in fixed-target mode will cover a simlar region relative to existing data but the observables available will offer more insight into the nuclear gluon distribution

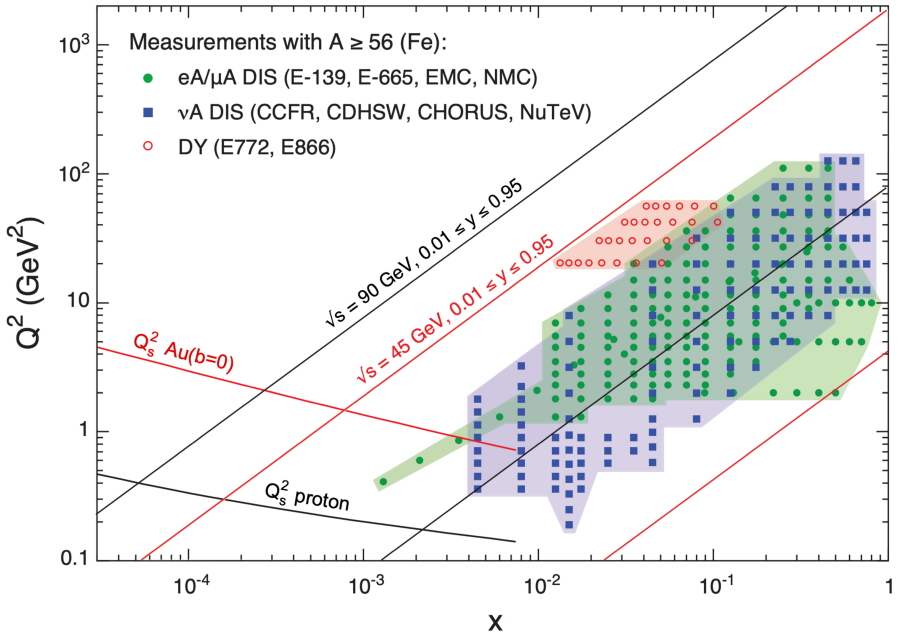

Energy Loss

.

Energy loss in medium

Based on the relative size of the formation time of a soft radiated gluon compared to the medium it travels through, the matter the gluon scatters with can be seen as incoherent scattering centers (Bethe-Heitler); partially coherent, with a group of scattering centers acts like a single radiator (LPM regime); fully coherent (FCEL) where all scattering centers acts like a radiation source; and Bertsch-Gunion regime (BG-like) where initial state interactions can partially cancel radiation effects

	ΔE	Observables	Systems	Facilities
Initial state LPM	$\hat{q}\,L^2\,\ln E$	Drell-Yan	$h+A$	E906, COMPASS
Final state LPM	$\hat{q}\,L^2\,\ln E$	h, jets	$e+A$	CLAS, HERMES, EIC
FCEL	$(\hat{q}\,L)^{1/2}\,(E/M_T)$	h, jets	$h+A$	SPS, FNAL, RHIC, LHC
BG-like	$f(\hat{q}\,L)L\,E$	high x_F Drell-Yan, h, jets	$h+A$	FNAL, RHIC, LHC

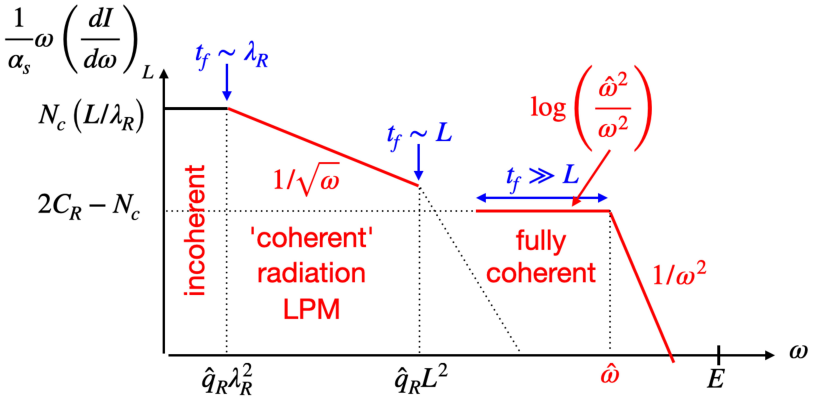

Transport Coefficient $\hat{q}$

Strength of induced gluon radiation governed by transport coefficient $\hat{q}$, related to the gluon distribution evaluated at the momentum scale $Q^2 \sim \Delta p_T^2$.

$$\hat{q} \equiv \frac{\tilde{\mu}^2}{\lambda} = \frac{4\pi^2\,\alpha_s\,C_R}{N_c^2-1}\,\rho\,xg\big(x,Q^2\big)$$

$\hat{q}$ can be determined from analyses of transverse momentum broadening, $\Delta p_T^2 = \langle p_T^2 \rangle_{hA} - \langle p_T^2 \rangle_{hp}$, related to multiple parton scattering

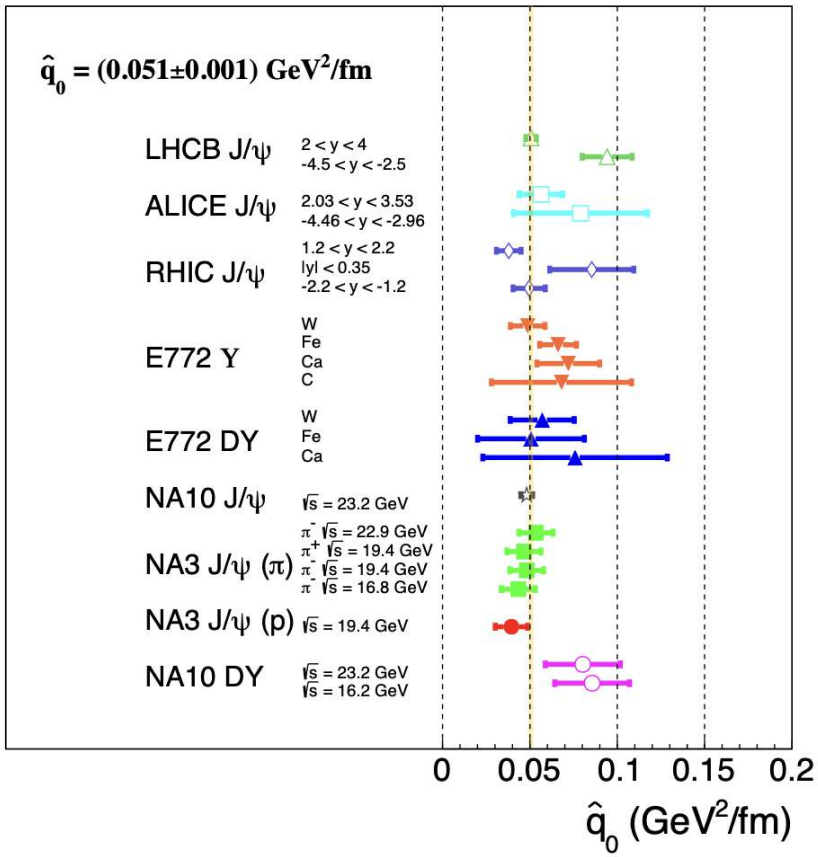

Using J/ψ Data to Pin down Nuclear Gluon PDF

The nPDF uncertainty on the low x gluon distribution can be large just based on DIS and DY data

The J/ψ is predominantly produced by gluons but is subject to other effects

Including J/ψ data can significantly reduce the uncertainties but the amount of low x shadowing depends on whether or not energy loss is taken into account

Such analyses may be unlikely to be improved in the high x range of the fixed-target mode but that may depend on the nPDF (EPPS21 has large uncertainties in this region also, unlike the nNNPDF distributions)

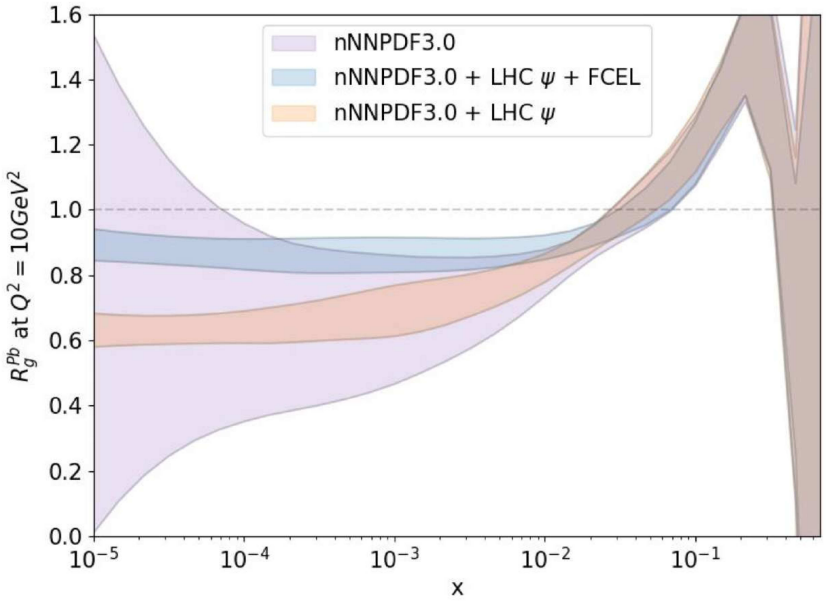

Energy Loss: Observables

1. **Drell-Yan at high x_F – well suited for studies of LPM energy loss**
2. **J/ψ production in $e+A$ and $p+A$ – FCEL depends on the color structure of the partonic process and is thus not universal; comparison of $e+A$ and $p+A$ J/ψ production could test this non-universality**

$$\begin{aligned} R_{eA}^{J/\psi}(x) &\simeq R_{eA}^{\mathbf{nPDF}}(x) \approx R_g^A(x); \\ R_{pA}^{J/\psi}(y,x_2) &\simeq R_{pA}^{\mathbf{nPDF+FCEL}}(y,x_2) \\ &\approx R_g^{\mathbf{A}}(x_2) \times R_{pA}^{\mathbf{FCEL}}(y,x_2)\,. \end{aligned}$$

3. **$R_{pA}^{J/\psi}/R_{pA}^{\mathrm{DY}}$ at forward rapidity or large x_F – this ratio should be above unity for nPDF effects alone but smaller than unity for FCEL**
4. **p_T broadening – useful for extracting $\hat{q}$ and constraining energy loss in Drell-Yan, quarkonium production, or SIDIS**
5. **Light hadrons and heavy flavors at large x_F – Bertsch-Gunion type energy loss can suppress energetic final-states at large x_F**

Absorption and Comovers: Final-State Effects

.

Absorption by Nucleons

.

Is Absorption Important for J/ψ Production?

Different methods used to extract an absorption cross section reach different conclusions about the size of $\sigma_{\rm abs}$

The absorption cross section is related to the production model (singlet, octet, or some combination) and to whether or not other CNM effects are included

Originally, absorption was a 'catch all' to cover all effects with a single, kinematics dependent parameter α, $\sigma_{pA} = \sigma_{pp} A^{\alpha}$

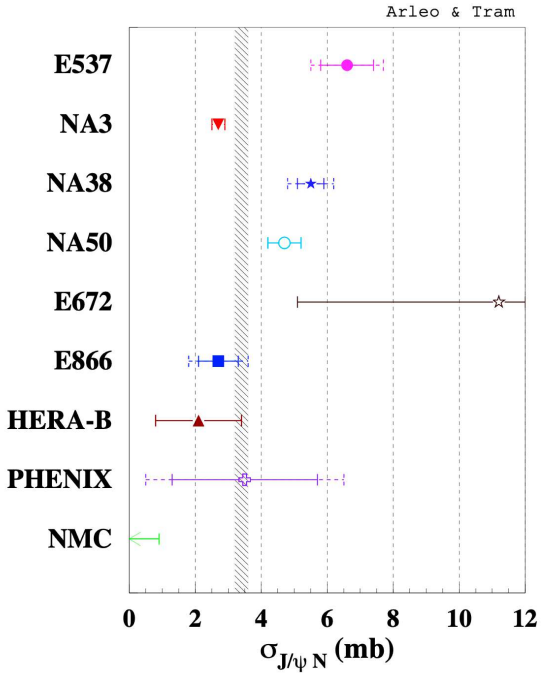

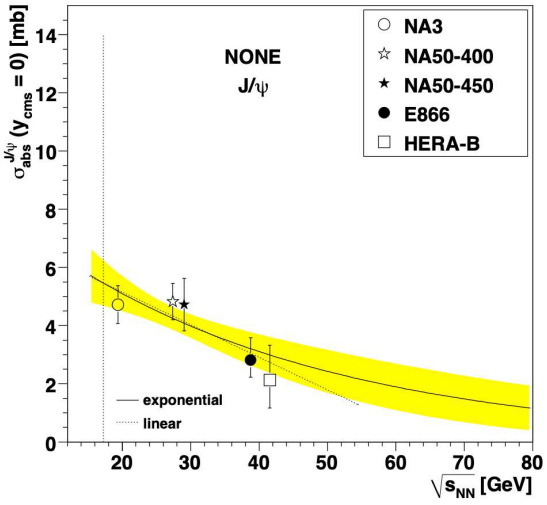

Interplay of nPDF Effects and Absorption

Depending on x values probed, shadowing can enhance or reduce absorption cross section needed to describe data

Absorption alone always gives less than linear A dependence ($\alpha < 1$)

For SPS energies, $17.3 \leq \sqrt{S} \leq 29$ GeV, rapidity range covered is in EMC and antishadowing region, $\alpha > 1$ with no absorption

Adding shadowing to absorption in the SPS energy region requires a larger absorption cross section is needed to maintain agreement with data

For $\sqrt{S} \geq 38$ GeV, x in shadowing regime, thus $\alpha < 1$ with shadowing alone in forward region, reducing needed absorption cross section to $\sigma_{\rm abs} \sim 0$ at the LHC

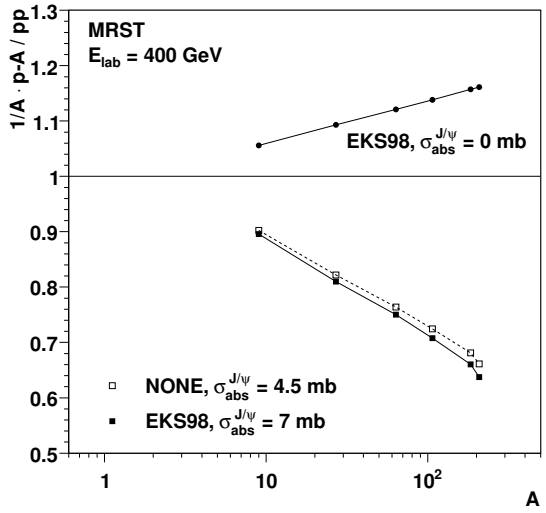

Figure 2: **(Left) Illustration of the interplay between shadowing and absorption. [C. Lourenco, H. K. Woehri and RV, JHEP 0902 (2009) 014.]**

$\sigma_{\rm abs}$ Grows with Time $c\bar{c}$ Spends Traversing Nucleus

At lower fixed-target energies J/ψ (longer $\tau = L/\gamma$) dominated by conversion of color octet $c\bar{c}$ pair to color singlet J/ψ by gluon emission (left)

$$\sigma_{\rm abs}(\tau) = \sigma_1 \left(\frac{\sqrt{s}}{10\ GeV}\right)^{0.4} \left(\frac{r_{c\bar{c}}(\tau)}{r_{\rm J/\psi}}\right)^2 \qquad r_{c\bar{c}}(\tau) = r_0 + v_{c\bar{c}}\tau \text{ for } r_{c\bar{c}}(\tau) < r_\psi$$

At higher energies (shorter τ) conversion occurs outside target

In fixed-target mode, the J/ψ stays in nuclear matter over most of x_F range (right)

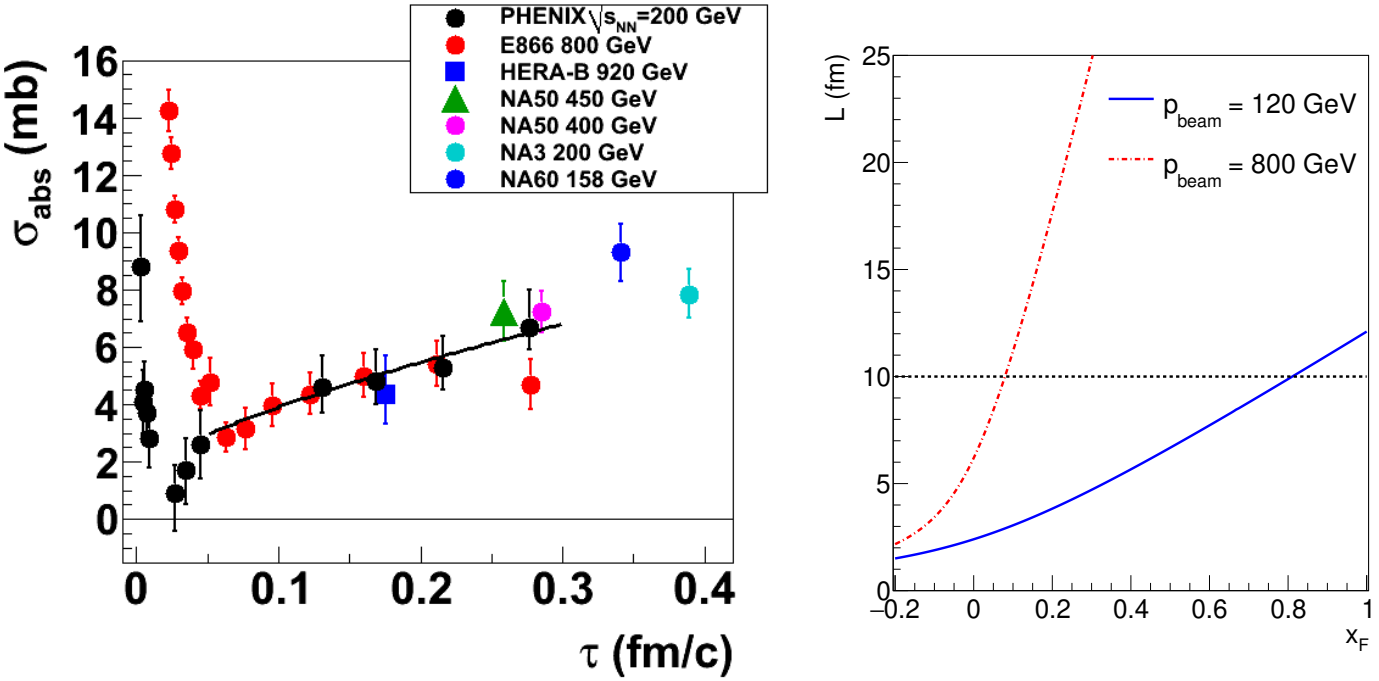

Figure 3: (Left) The effective $c\bar{c}$ breakup cross section as a function of the proper time spent in the nucleus, τ. The values were extracted from PHENIX $\sqrt{s_{NN}} = 200$ GeV d+Au data after correction for shadowing using EPS09 and from fixed-target p+A data measured by E866 at 800 GeV, by HERA-B at 920 GeV, by NA50 at 450 GeV and 400 GeV, by NA3 at 200 GeV, and by NA60 at 158 GeV. In all fixed-target cases, the EKS98 parameterization was used. The curve is calculated based on octet-to-singlet conversion inside the nucleus. [D. McGlinchey, A. D. Frawley and RV, Phys. Rev. C **87** (2013) 054910.] (Right) Path length through the nucleus as a function of x_F for beam momenta of 120 (blue) and 800 (red) GeV.

Comover Interaction Model

.

Comover Interaction Model, Ferriero *et al.*

Comover interaction rate

$$\Gamma^{\mathcal{Q}}(T) = \int_{E^{Q}_{\rm thr}}^{\infty} dE^{\rm co}\, \sigma^{\mathcal{Q}}_{\rm geo} \left(1 - \frac{E^{\mathcal{Q}}_{\rm thr}}{E^{\rm co}}\right)^{n} \frac{\rho^{\rm co}}{e^{E^{\rm co}/T_{\rm eff}} - 1} \tag{1}$$

$E^{Q}_{\rm thr} = M_Q + m_{\rm co} - 2M_H$ **where** $Q = c$ **or** b, $H = D$ **or** B, $E^{\rm co} = \sqrt{p^2 + m^2_{\rm co}}$ **with** $m_{\rm co} = 0$ **for gluons and 140 MeV for pions;** ρ^0 **is the transverse density of comovers, proportional to the multiplicities;** $\sigma^0_{\rm geo} \simeq \pi r^2_Q$**; the power** n **is between 0.5 and 2 and** $T_{\rm eff} \simeq 200 - 300$ **MeV**

Dissociation of quarkonium by comover interactions as a function of time

$$\tau \frac{{\rm d}\rho^{\mathcal{Q}}}{{\rm d}\tau}\,(b,s,y) \;=\; -\sigma^{{\rm co}-\mathcal{Q}}\,\rho^{\rm co}(b,s,y)\,\rho^{\mathcal{Q}}(b,s,y)\;, \tag{2}$$

$\sigma^{{\rm co}-Q}$ **is the energy-averaged quarkonium-comover interaction cross section**

The densities of comovers and quarkonium are $\rho^{\rm co}$ **and** ρ^{Q} **respectively**

Integrating over time τ **from** τ_i **to** τ_f **gives the survival probability**

$$S^{\rm co}_{\mathcal{Q}}(b,s,y) \;=\; \exp\Big\{ -\sigma^{{\rm co}-\mathcal{Q}}\,\rho^{\rm co}(b,s,y)\,\ln\Big(\rho^{\rm co}(b,s,y)/\rho_{pp}(y)\Big)\Big\} \tag{3}$$

Shadowing is included but other cold matter effects are not

The different sizes of $\sigma^{{\rm co}-Q}$ **for** $Q = J/\psi$ **and** ψ**(2S) result in stronger comover dissociation for** ψ' **than** J/ψ

It has been shown that the A **dependence of comover interactions and nucleon absorption are effectively the same (Gavin and Vogt)**

Comovers Affect J/ψ and $\psi(2S)$ Differently

$\sigma^{\mathrm{co}-Q}$ fixed low-energy experimental data: $\sigma^{\mathrm{co}-J/\psi} = 0.65$ mb and $\sigma^{\mathrm{co}-\psi(2\mathrm{S})} = 6$ mb

Larger effect of comovers near the nucleus ($-y_{\mathrm{cms}}$), would affect more of the y region at lower energies but with lower comover densities

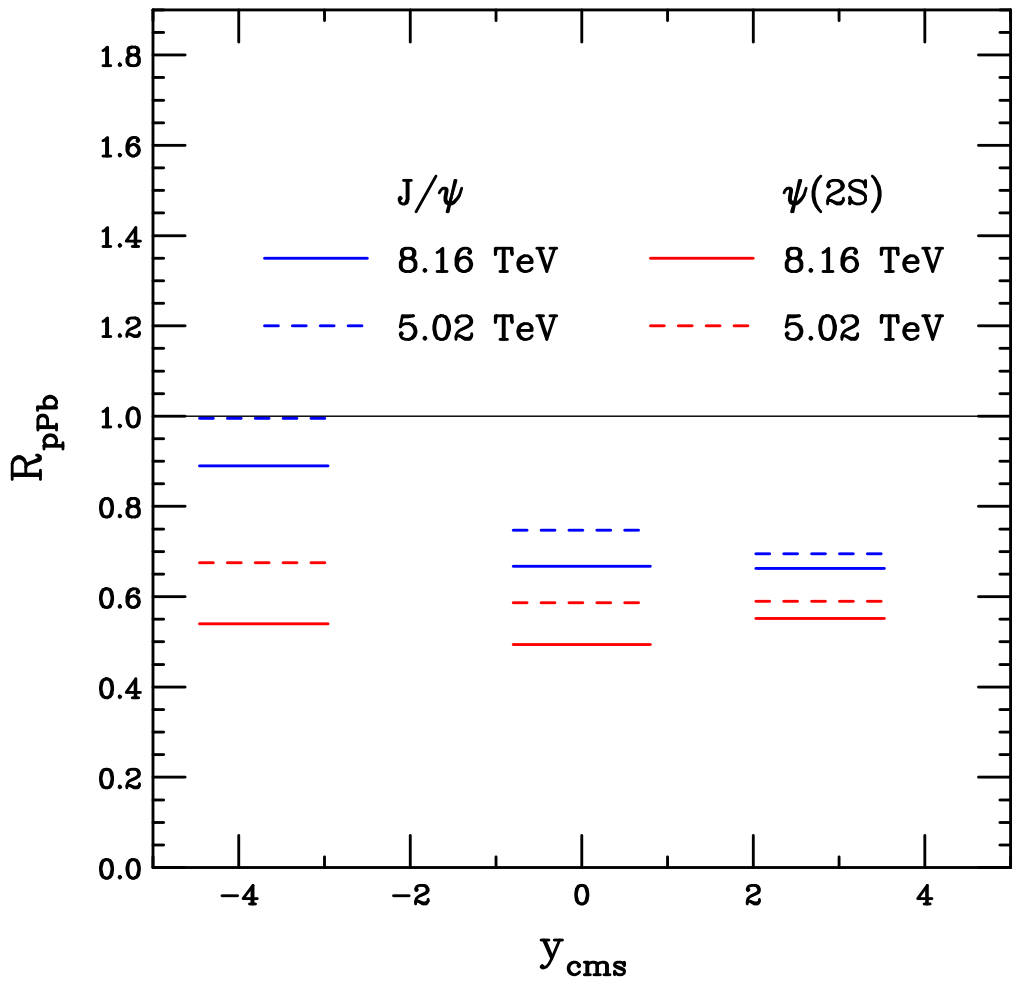

Figure 4: **The rapidity dependence of J/ψ and ψ(2S) production in the comover interaction model at 5.02 and 8.16 TeV. The EPS09 LO shadowing parameterization is also included. From Elena Ferreiro, in NPA 972 (2018) 18, arXiv:1707.09973 [hep-ph].**

Absorption and Comovers: Observables

1. **Double ratios of quarkonium states, $R^{Q\overline{Q}_i}/R^{Q\overline{Q}_j}$ – this ratio should be independent of nPDF and energy loss effects and so could isolate absorption effects for $t_{\rm form} \leq L$ where there are few comovers, as in this case**
2. **Comover production should decrease or vanish at the lower energy range of where the J/ψ can be produced in fixed-target mode**
3. **$R^{J/\psi}$ vs. R^{χ_c} – differences in the color state at production could result in different absorption cross sections**
4. **Hadron production in SIDIS in $e+p$ vs. $e+A$ – absorption effects can be isolated in regions were energy loss and nPDF effects are small**

Impact Parameter Dependent nPDF Effects

.

Impact Parameter Dependent nPDFs

.

Impact parameter dependenct nPDFs first proposed in PRC 56, 2726 (1997)

Two parameterizations chosen, one with shadowing proportional to the nuclear density and the other proportional to the nuclear thickness at the collision point

Both are normalized such that $(1/A)\int d^2b dz \rho(s) S^i(A,x,Q^2,\vec{b},z) = S^i(A,x,Q^2)$

$$
\begin{aligned}
S^i_{\rm WS}(A,x,Q^2,\vec{b},z) &= 1 + N_{\rm WS}(S^8(A,x,Q^2)-1)\frac{\rho(\vec{b},z)}{\rho_0} \\
S^i_{\rm R}(A,x,Q^2,\vec{b},z) &= \begin{cases} 1 + N_{\rm R}(S^i(A,x,Q^2)-1)\sqrt{1-(b/R_A)^2} & b \le R_A \\ 1 & b > R_A \end{cases}
\end{aligned}
$$

McGlinchey *et al.* **(PRC 87 (2013), 054910) tried two forms for the impact parameter dependence of** J/ψ **after these original forms proved too weak for PHENIX d+Au data:**

1) EPS09s keeps powers $n = 1 \cdots 4$ **for** A**-independent coefficients**

$$S^i(A,x,Q^2,\vec{b},z) = 1 - (1 - S^i(A,x,Q^2)\,)\left(\frac{T_A^n(b)}{a(n)}\right)$$

2) Step function with radius R **and diffuseness** d **left as free parameters**

$$S^i(A,x,Q^2,\vec{b},z) = 1 - \left(\frac{1 - S^i(A,x,Q^2)}{a(R,d)(1+\exp((b-R)/d))}\right)$$

Centrality Dependence of CNM on in d+Au Collisions

Shadowing appears to be concentrated in core of Au nucleus $R = 2.4$ fm, $d = 0.12$ fm

At higher energies, the entire nucleus may act as a "hot spot" with $R \sim R_A$

At low fixed-target energies, hot spots could have smaller values of R and d, *i.e.* $R \sim r_0 = 1.2$ fm, stronger short-range coherence

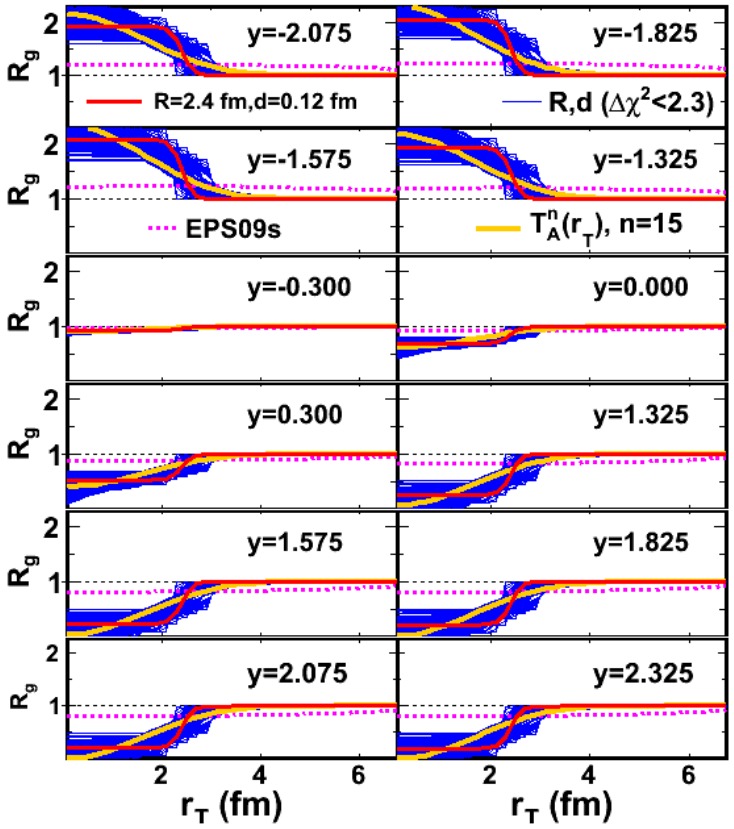

Figure 5: **Transverse radius dependence of gluon shadowing ratio R_g (based on EPS09 NLO) for the PHENIX d+Au rapidity bins. The results compare b-dependence based on path length through the nucleus, $T_A(b)$, and a sharp surface with radius and diffuseness parameters. (PRC 87 (2013), 054910)**

Intrinsic Heavy Flavor Production

.

What are Intrinsic Heavy Flavors?

Proton wavefunction can be expanded as sum over complete basis of quark and gluon states: $|\Psi_p\rangle = \sum_m |m\rangle\, \psi_{m/p}(x_i, k_{T,i}, \lambda_i)$

$|m\rangle$ **are color singlet state fluctuations into Fock components** $|uud\rangle$, $|uudg\rangle \cdots |uudc\overline{c}\rangle$

The intrinsic Q **fluctuations can be freed by a soft interaction if the system is probed during the time** $\Delta t = 2p_{\rm lab}/M^2_{c\overline{c}}$ **that the fluctuations exist**

Dominant Fock state configurations have minimal invariant mass, $M^2 = \sum_i m^2_{T,i}/x_i$, **where** $m^2_{T,i} = k^2_{T,i} + m^2_i$ **is the squared transverse mass of parton** i **in the state; corresponds to configurations with equal rapidity constituents**

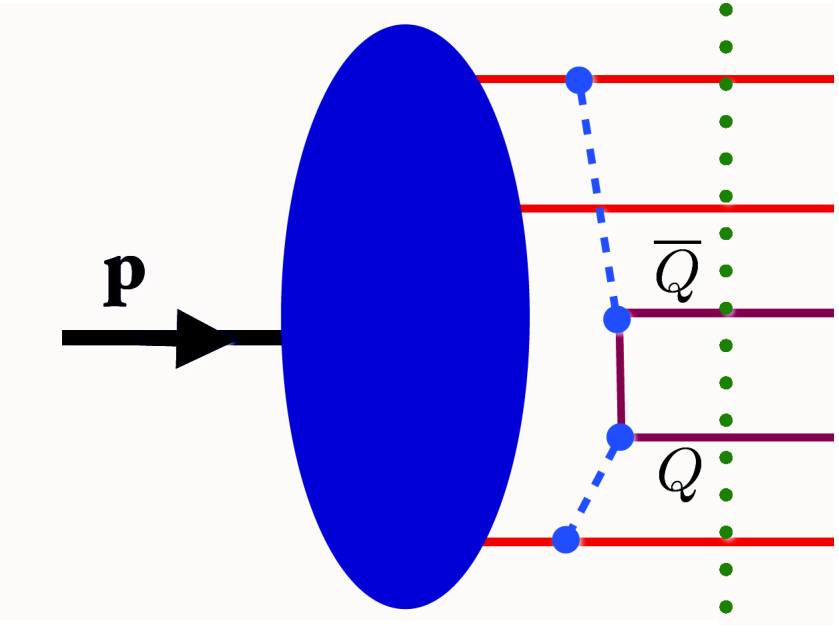

Production by Intrinsic Heavy Quarks

Probability distribution of five-particle Fock state of the proton:

$$dP_{\mathrm{iQ}\,5} = P^0_{\mathrm{iQ}\,5} N_5 \int dx_1 \cdots dx_5 \int dk_{x\,1} \cdots dk_{x\,5} \int dk_{y\,1} \cdots dk_{y\,5} \frac{\delta(1-\sum_{i=1}^5 x_i)\delta(\sum_{i=1}^5 k_{x\,i})\delta(\sum_{i=1}^5 k_{y\,i})}{(m_p^2 - \sum_{i=1}^5 (\widehat{m}_i^2/x_i))^2}$$

$i = 1, 2, 3$ are u, u, d light quarks, 4 and 5 are Q and $\overline{Q}$, N_t normalizes the probability to unity and P^0_{ic} scales the normalized probability to the assumed intrinsic charm content: 0.1%, 0.31% and 1% are used to represent the range of probabilities assumed previously (based on original Brodsky *et al.* model, intrinsic bottom content would be approximately an order of magnitude smaller

The intrinsic charm cross section is determined from soft interaction scale breaking coherence of the Fock state, $\mu^2 = 0.1$ GeV^2

$$\sigma^{\mathrm{ic}}_{pp} = P_{\mathrm{ic}\,5} \sigma^{\mathrm{in}}_{pN} \frac{\mu^2}{4\widehat{m}_c^2}$$

The cross sections from intrinsic charm are then obtained by multiplying by the normalization factor for the CEM to the J/ψ

$$\sigma^{\mathrm{ic}}_{pp}(J/\psi) = F_C \sigma^{\mathrm{ic}}_{pp} \quad \sigma^{\mathrm{ic}}_{pA} = \sigma^{\mathrm{ic}}_{pp} A^{\beta} \quad , \beta = 0.71 \ \ (\mathrm{NA3})$$

Other assumptions of intrinsic charm distributions in the nucleon are the meson cloud model ($c(x) \neq \overline{c}(x)$) and a sea-like distribution ($c(x) = \overline{c}(x) \propto \overline{d}(x) + \overline{u}(x)$)

Recent and Forthcoming Fixed-Target Experiments Ideal for IC Studies

Many previous experiments studied J/ψ production off nuclear targets at proton beam energies from 158 to 920 GeV, several used to get a baseline for $A + A$ collisions; those that covered large x_F saw a larger suppression of production off nuclear targets at higher x_F

SeaQuest: Took data with a 120 GeV proton beam on p, d, C, Fe, and W targets, covered forward region, $0.4 < x_F < 0.95$ and $p_T < 2.3$ GeV; J/ψ data not published yet but should report nuclear suppression factor, $pA/p\mathrm{d}$

SMOG: Gas jet target in LHCb, J/ψ and D^0 measured at backward rapidity in the fixed-target center of mass, data so far at: $p + \mathrm{Ne}$ at $\sqrt{s_{NN}} = 68.5$ GeV; $p + \mathrm{He}$ at $\sqrt{s_{NN}} = 86.6$ GeV; and $p + \mathrm{Ar}$ at $\sqrt{s_{NN}} = 110.4$ GeV

NA60+: proton beams at $p_{\mathrm{lab}} = 40$, 80, and 120 GeV, nuclear targets from Be to Pb

Calculations and comparison to data in the following from R. Vogt, arXiv:2101.02858, Phys. Rev. C 103, 035204 (2021); arXiv:2207.04347, Phys. Rev. C 106, 025201 (2022); arXiv:2304.03451, Phys. Rev. C 108, 015201 (2023)

SMOG J/ψ Results Compared to Calculations

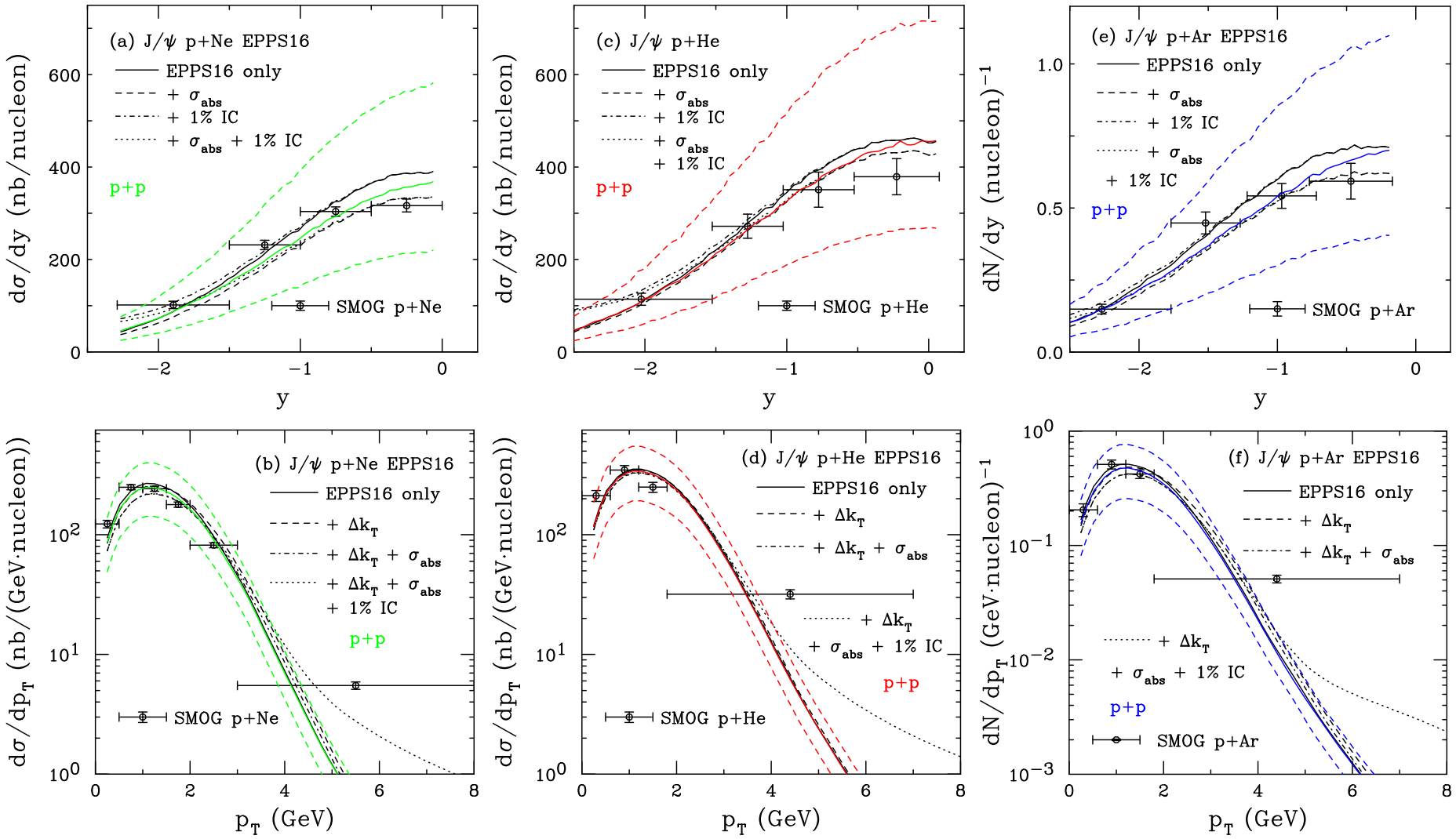

Figure 6: The J/ψ cross section as a function of y in (a), (c), (e) and p_T in (b), (d), (f) for $p+$Ne ($\sqrt{s_{NN}} = 68.5$ GeV) in (a) and (b); $p+$He ($\sqrt{s_{NN}} = 86.6$ GeV) in (c) and (d); and $p+$Ar ($\sqrt{s_{NN}} = 110.4$ GeV) in (e) and (f). The black curves are the $p+A$ calculations. The colored curves (solid and dashed) show the CEM $p+p$ calculations (no IC). The $p+A$ rapidity distributions are shown for EPPS16 only (solid); EPPS16 with absorption (dashed); EPPS16 and $P^0_{\rm ic\,5} = 1\%$ (dot-dashed); and EPPS16, absorption, and $P^0_{\rm ic\,5} = 1\%$ (dotted). The p_T distributions show EPPS16 only (solid); EPPS16 with k_T kick (dashed); EPPS16, absorption, and k_T kick (dot-dashed); and EPPS16, absorption, k_T kick and $P^0_{\rm ic\,5} = 1\%$ (dotted). The $p+$Ne data are from arXiv:2211.11645; the $p+$He and $p+$Ar data are from PRL **122**, 132002 (2019).

$p+p$ distributions as a function of y and p_T: With and Without Intrinsic Charm

All p_T calculations assume integration over all y, the intrinsic charm contribution would be overestimated if the contribution would be restricted to midrapidity – this effect becomes larger at higher energies, there would be no contribution to the midrapidity p_T distribution at all at RHIC and LHC energies

The strong energy dependence of the intrinsic charm contribution is evident; any pQCD nuclear effects would be quickly overwhelmed

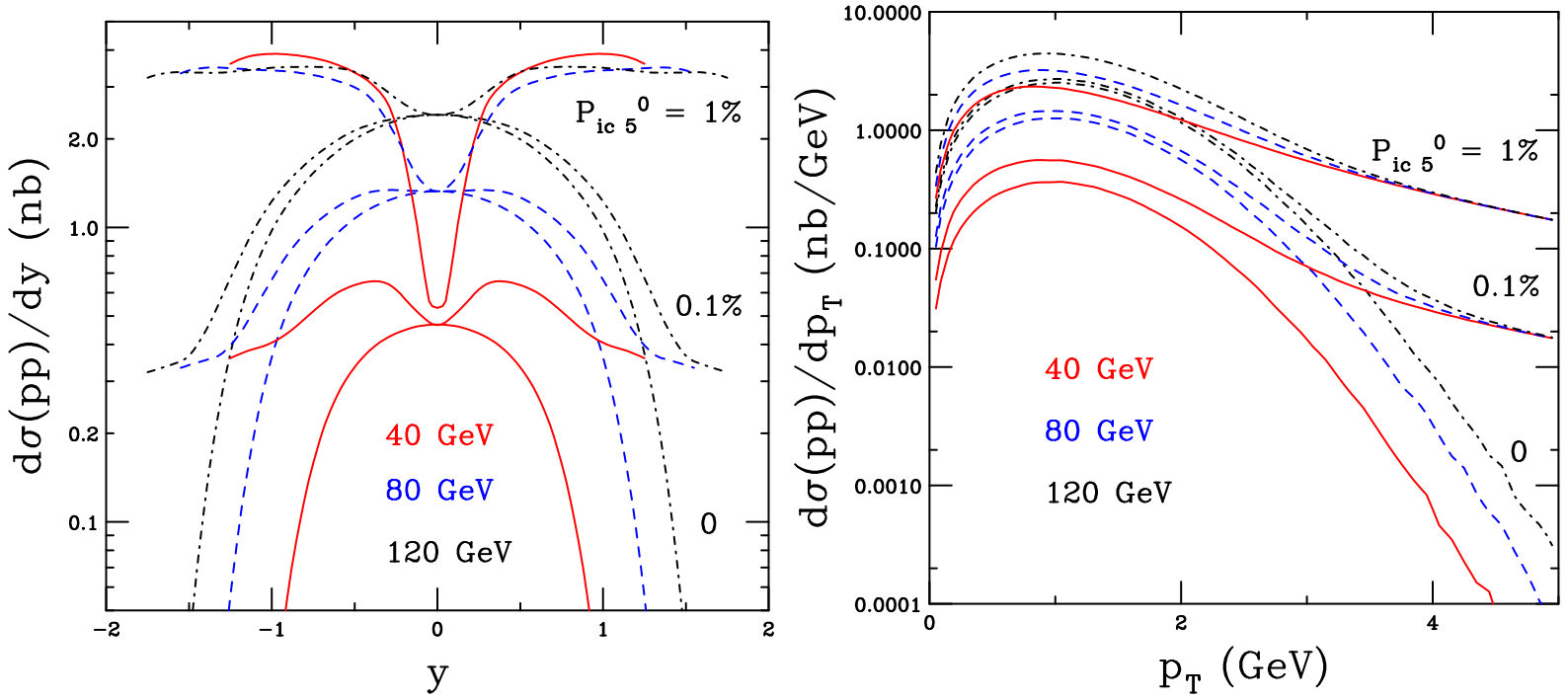

Figure 7: The nuclear modification factors for J/ψ production as a function of y (left) and p_T (right) in $p+p$ collisions with $P^0_{\rm ic\,5} = 0\%$ (bottom curves) 0.1% (middle curves) and 1% (upper curves). The solid red, blue dashed and black dot-dashed curves are for $p_{\rm lab} = 40$, 80 and 120 GeV respectively.

Observables for Centrality Dependent nPDFs and Intrinsic Heavy Flavors

1. **Impact parameter dependence of nPDFs – is the nucleus made up of shadowing hot spots or is shadowing uniform throughout the nucleus? PHENIX d+Au data suggested the former while ALICE data may suggest the latter. The lower the energy the smaller the potential hot spot for shadowing.**
2. **Intrinsic heavy flavors – at these lower fixed-target center of mass energies, intrinsic charm effects, if present, should be striking**

CNM Effects in the EIC Fixed-Target Setup

In this energy range, x_2 is large, no saturation expected

J/ψ absorption by nucleons should be large

If intrinsic charm is present, then it should be clearly visibile in the fixed-target energy range

Some of the $p+A$ data, particularly for charged pions, could align well with needs of the space program

Finally, $p+A$ measurements in this energy range will provide a so far missing baseline for $A+A$ collisions in the STAR Beam Energy Scan II program

The breadth of the program will depend on the type and number of targets, it may not realize its full potential until a second detector is designed with the program in mind